Acta Oceanol. Sin., 2019, Vol. 38, No. 3, P. 17–25
https://doi.org/10.1007/s13131-019-1395-5
http://www.hyxb.org.cn
E-mail: hyxbe@263.net

The *in situ* observation of modelled sea ice drift characteristics in the Bohai Sea

Yu Yan[1, 2], Wei Gu[1, 2], Yingjun Xu[1, 2*], Qian Li[1, 2]

[1] Key Laboratory of Environmental Change and Natural Disaster of Ministry of Education, Faculty of Geographical Science, Beijing 100875, China

[2] Academy of Disaster Reduction and Emergency Management, Beijing Normal University, Beijing 100875, China

Received 5 January 2018; accepted 30 January 2018

Abstract

Sea ice drift is mainly controlled by ocean currents, local wind, and internal ice stress. Information on sea ice motion, especially *in situ* synchronous observation of an ice velocity, a current velocity, and a wind speed, is of great significance to identify ice drift characteristics. A sea ice substitute, the so-called "modelled ice", which is made by polypropylene material with a density similar to Bohai Sea ice, is used to complete a free drift experiment in the open sea. The trajectories of isolated modelled ice, currents and wind in the Bohai Sea during non-frozen and frozen periods are obtained. The results show that the currents play a major role while the wind plays a minor role in the free drift of isolated modelled ice when the wind is mild in the Bohai Sea. The modelled ice drift is significantly affected by the ocean current and wind based on the ice–current–wind relationship established by a multiple linear regression. The modelled ice velocity calculated by the multiple linear regression is close to that of the *in situ* observation, the magnitude of the error between the calculated and observed ice velocities is less than 12.05%, and the velocity direction error is less than 6.21°. Thus, the ice velocity can be estimated based on the observed current velocity and wind speed when the *in situ* observed ice velocity is missing. And the modelled ice of same thickness with a smaller density is more sensitive to the current velocity and the wind speed changes. In addition, the modelled ice drift characteristics are shown to be close to those of the real sea ice, which indicates that the modelled ice can be used as a good substitute of real ice for *in situ* observation of the free ice drift in the open sea, which helps solve time availability, safety and logistics problems related to *in situ* observation on real ice.

Key words: Bohai Sea, modelled ice, *in situ* observation, sea ice drift

Citation: Yan Yu, Gu Wei, Xu Yingjun, Li Qian. 2019. The *in situ* observation of modelled sea ice drift characteristics in the Bohai Sea. Acta Oceanologica Sinica, 38(3): 17–25, doi: 10.1007/s13131-019-1395-5

1 Introduction

Sea ice drift, a crucial part of oceanology studies, is a complex form of movement under the influence of a variety of forces, especially controlled by ocean currents and local wind. The synchronous observation of the ice velocity, the current velocity, and the wind speed, is of great significance to identify ice drift characteristics (Simizu et al., 2014; Timmermans et al., 2011; Wake et al., 1987; Wu et al., 2005). At present, methods obtaining synchronous data mainly include the drifting buoy observations of multi-year ice in polar regions and experimental studies of modelled ice in indoor tanks.

The main method used for the *in situ* observations of ice drift in the perennial ice zone is the application of drifting buoys, which is direct and accurate (King, 2003; Richter-Menge et al., 2006; Timmermans et al., 2011). Researchers place the buoy onto multi-year ice through drilling or air-launching and then receive ice trajectory and other simultaneous observation data by satellite transmission. Timmermans et al. (2011) collected a floe velocity, a barometer pressure, and the current velocity using an autonomous ice-based observatory equipped with an ice-mass balance and autonomous ocean flux buoys in the Eurasian Basin per day via the Iridium Satellite between April and November 2010. King (2003) deployed three compact air-launched ice beacons on ice in the Bellingshausen Sea, Antarctica, and collected the sea ice location and the barometric pressure using the Argos satellite every 1–2 h for half a month to 3 months. Richter-Menge et al. (2006) drilled an approximately 1 m deep hole in undeformed and multi-year ice near the North Pole and in the Beaufort Sea and then installed a tube attached to an autonomous ice buoy transmitting the trajectory and barometric pressure data every 1–2 h using the Argos satellite system.

Indoor tanks are mainly used for the application of modelled ice to record the ice drift characteristics. Murray et al. (1983) conducted an experiment to determine the maximum instantaneous velocities of a range of modelled ice casted by paraffin wax with cylindrical, spherical, and cubical shapes in regular waves in the wave tank. Wake et al. (1987) investigated the transport of isolated modelled ice made of low-density polyethylene with different dimensions by wind, wave, and drift currents in a wind–wave tank. Huang et al. (2011) determined the drift of modelled ice made of polyethylene with different shapes (square, circular and elliptical) at two different submergences in a wave tank.

The Bohai Sea is the southernmost seasonal frozen sea in the Northern Hemisphere. The frozen period is short in the Bohai

Foundation item: The National Natural Science Foundation of China under contract No. 41571510; the Fundamental Research Funds for the Central Universities of China under contract No. 2014KJJCB02.
*Corresponding author, E-mail: xyj@bnu.edu.cn

Sea and the majority of the existing sea ice is drift ice, which is thin and easily breaks (Gu et al., 2013). However, an *in situ* buoy which is expensive and non-recyclable is not applicable to the Bohai Sea where is full of first-year ice. The research on the sea ice drift in the Bohai Sea mainly concentrated on non-contact measurements, such as satellite remote sensing observations and radar monitoring, in recent years. Ji et al. (2013) derived ice drift vector fields and the ice velocities of feature points every 5 min at the JZ 20-2 oil and gas platform in the Liaodong Gulf using radar digital images. Lang et al. (2014) computed daily 1 h sea ice drift vector fields in the Bohai Sea from a geostationary ocean color imager and derived current and wind data from weather research and forecasting and regional ocean models, respectively. However, remote sensing and radar methods generally can only obtain the information on the sea ice drift but have difficulties in accessing the ice velocity, the current velocity, and the wind speed, simultaneously. Very few studies focused on the *in situ* synchronous observation of ice–current–wind. Only Fukamachi et al. (2011) investigated the sea ice drift characteristics in the Sea of Okhotsk using an *in situ* synchronous observation, which was composed of an acoustic Doppler flow profiler (ADCP) and a nearby coastal weather station. Here the ice and water velocities were obtained from the ADCP and the wind data were measured by the weather station during the winters of 1999–2001. The modelled ice used in the indoor tank, nevertheless, is limited by the boundary of the tank and the size of the modelled ice, which cannot reflect the field situation. Little attention has been devoted to the study of modelled ice in field experiments. Considering the limits mentioned above, we developed an *in situ* synchronous observation of ice–current–wind based on modelled ice to make a novel solution. On the one hand, it could help to understand the characteristics of the sea ice drift and provide key input parameters for the numerical simulation of the sea ice drift. On the other hand, it solved the problems such as limited time for observations due to short frozen periods and high costs and safety of ice navigation.

In this paper, the free drift experiments of modelled ice in the open sea in the Liaodong Gulf and the Bohai Gulf in the Bohai Sea were carried out during the non-frozen period. A comparative free drift experiment between modelled ice and real sea ice was conducted in the frozen period in the Liaodong Gulf. The paper is organized as follows: in Section 2, an experimental setup, time, and place are introduced; in Section 3, the primary results on the modelled ice drift characteristics in the Bohai Sea, the relationship among ice–current–wind, the comparison of different densities and thicknesses and the comparison of the ice drift between modelled ice and real ice are presented. The relevant discussion is also provided in this section. The main conclusions are summarized in Section 4.

2 Materials and methods

2.1 *Experimental design*

In the present study, a free drift field experiment of modelled ice, similar to the Bohai Sea ice, was performed during the non-frozen period and the trajectories of modelled ice, the current velocity, and the wind speed were recorded simultaneously. The characteristics of the modelled ice drift were then described and the relationship between ice–current–wind was established. In addition, the difference of the ice drift between modelled and real sea ice was determined using a comparable experiment in the frozen period.

2.2 *Modelled ice design*

The mechanical properties, size, and shape of sea ice are quite varied, which can significantly affect the ice drift (Murray et al., 1983). The density is one of the most important mechanical properties. The density of sea ice in the Bohai Sea ranges from 0.74 to 0.92 g/cm^3, with a common density of 0.85 g/cm^3 (Lin et al., 2010). Polypropylene with a density close to the sea ice in the Bohai Sea was used to model the isolated ice by comparing paraffin (0.89–0.91 g/cm^3) (Bai et al., 2017; McGovern and Bai, 2014; Murray et al., 1983), wood (0.72 g/cm^3) (Huang and Law, 2013), and high polymer materials (0.80–0.92 g/cm^3) (Huang et al., 2011; Meylan et al., 2015; Wake et al., 1987). Two thicknesses, 4.0 and 7.0 cm, were used to create different model ice. The shape of the modelled ice was selected based on common isolated sea ice (ellipse). In addition, for a modelled ice morphology close to that of real ice with a rough bottom, grooves were created to increase the roughness of polypropylene. The dimensions of the modelled ice used in the experiments are listed in Table 1; the design diagram and physical map of the modelled ice are shown in Fig. 1.

2.3 *Integrated observation system*

To accurately determine the ice drift characteristics, the simultaneous observations of ice-current-wind by an integrated observation system (Fig. 2) consisting of an automatic identification system (AIS), the ADCP, and weather station were indispensable. The trajectories of modelled ice were obtained by the AIS, which was an effective tool for maritime management (Robards et al., 2016). During the experiments, the signal transmitter of the AIS was placed in the center of the modelled ice and the antenna was placed vertically, 0.50 m above the sea level (Fig. 2). The AIS (ICOM, MAX-5000), which consisted of an AIS transponder, a receiving antenna, and a computer, received the broadcasted signal and logged the trajectory of the modelled ice every minute on land. Then the ice velocity was calculated by the observation data from the AIS. The AIS accuracy was 0.000 1′, thus the error in calculating the ice velocities was approximately 0.21 cm/s. The current velocity was measured by an upward-looking ADCP (TRDI, WHS-1200 Workhorse) using the surface-track mode. Its sampling interval was 1 min and the depth cell size was 0.5 m. The number of depth cells was set to 20. And the velocity in 2nd cell below surface was selected to represent the surface current since the current measured by the ADCP in the approximately 5% depth below surface (1st cell) had large errors due to the side-lobe reflections. The accuracy of the velocity was ±0.25% of water velocity relative to ADCP, ±2.5 mm/s, and the velocity resolution is 1 mm/s. The sea surface wind data were measured by the weather station (Kestrel, NK 5500) placed on the power-off vessel following the modelled ice with 3.0 m height

Table 1. Dimensions of modelled ice used in the experiment

No.	Density/g·cm^{-3}	Thickness/cm	Shape (ellipse)		Volume/cm^3	Mass/kg
			Major axis/cm	Minor axis/cm		
A	0.91	4.0	200.0	150.0	9.43×10^4	85.77
B	0.81	7.0	200.0	150.0	1.65×10^5	133.60
C	0.91	7.0	200.0	150.0	1.65×10^5	150.09

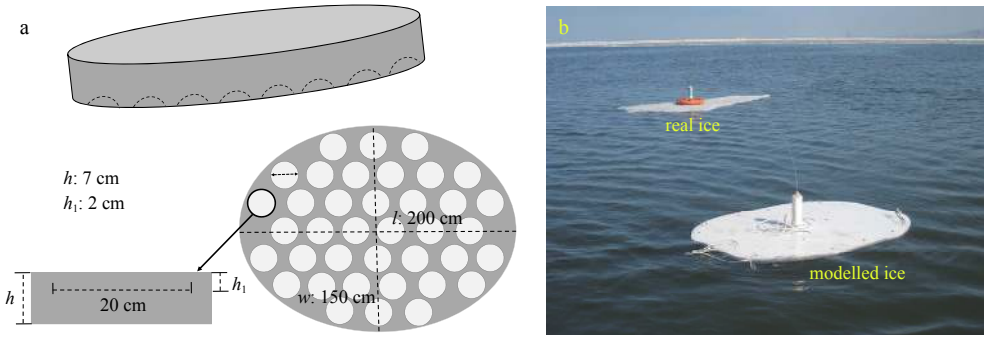

Fig. 1. Design diagram (a) and physical map (b) of the modelled ice, in which *l*, *w* and *h* is the length, width and height of the modelled ice, respectively.

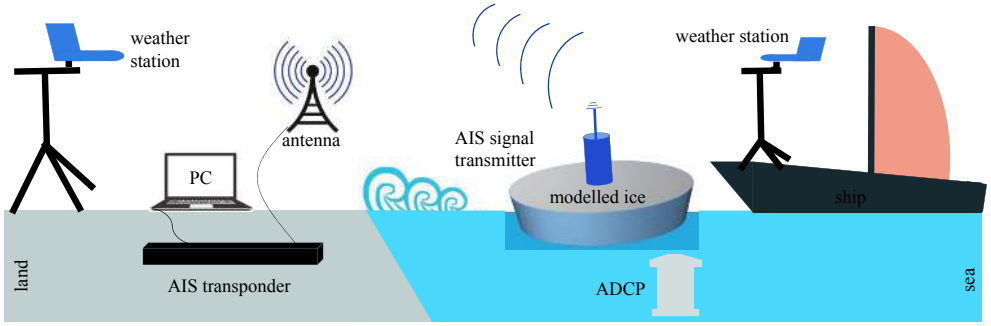

Fig. 2. Schematic of the integrated observation system.

above the sea level every 1 min. Meteorological data on land were also measured by the weather station every 1 min.

Notably, the wind direction was recorded as 0° at the weather station when the wind blew from the north to the south. While the current direction was recorded as 0° in the ADCP when the sea water flowed from the south to the north. The ice-drift direction was recorded in the same way as the current. To unify the record of the direction of ice, current and wind, we defined that the wind direction was 0° when it blew from the south to the north while the instrument was recorded as 180°. Therefore, after obtaining the wind data measured by the weather station, the wind direction needs to be converted before carrying out the analysis.

2.4 *Location and experiment time*

Bohai Sea ice is mainly concentrated in the Liaodong Gulf and the Bohai Gulf. The Liaodong Gulf is the northernmost frozen sea with the most serious ice conditions and longest frozen period in China (Liu et al., 2013), which is representative for sea ice in the Bohai Sea. In the Liaodong Gulf, we chose the open sea of the Bayuquan fishing port as the experiment site. The Bohai Gulf is another important frozen sea in the Bohai Sea with the Tianjin, Qinhuangdao, and Huanghua Ports along the coast. We chose the open sea of the Nanpaihe fishing port near Huanghua Port as the experiment site. *In situ* observations were conducted in the non-frozen and frozen periods, respectively. Early winter was selected for the experiment in the non-frozen period; at that time, the East Asian atmospheric circulation had converted to winter mode, which minimized the seasonal difference between non-frozen and frozen period experiments. The frozen period experiment was conducted in the ice melt period (February 2017), taking into account the safety of ice navigation.

In addition, the seabed topography at the experimental site was investigated before the study was carried out. Bayuquan is a rocky coast but the experimental sea area is flat; Nanpaihe is a typical silty coast with flat seabed terrain (Yan et al., 2016). Taking into account the spatial distribution of the ocean current and flat submarine terrain, the ocean current, with the ADCP as the center and 500 m radius within the sea range, can be considered to be uniform (Shi et al., 2016). In this study, the velocity profile measured by the ADCP was the vertical section of the fixed point. For more representative current measurements, the modelled ice was replaced near the ADCP before the next experiment was started.

The geographic elements of the study area are listed in Table 2 and the maps of the study area are shown in Fig. 3. The free drift experiments of the modelled ice during the non-frozen period were conducted in Bayuquan, the Liaodong Gulf, on 29 October 2016 and Nanpaihe Estuary, the Bohai Gulf, on 9 December 2016. The comparative free drift experiment between modelled and real sea ice during the frozen period was carried out in Bayuquan on 12 February 2017. However, Nanpaihe was ice-free in February due to the mild winter of 2016/2017; therefore, the planned comparative experiment in Nanpaihe could not be performed. Besides, the wind in Bayuquan and Nanpaihe based on daily data obtained from the website of the China Meteorological Data Sharing Service System (http://data.cma.cn/) was generally weak during the period October 2016 to February 2017. The mean wind speed in Bayuquan and Nanpaihe from October 2016 to February 2017 was 2.71 and 2.74 m/s, respectively.

3 Results and discussion

3.1 *Modelled ice drift characteristics and relationship with current and wind*

The trajectories of the modelled ice in Bayuquan and Nanpaihe during the non-frozen period are shown in Fig. 4 and the vectors of the ice velocity, the current velocity, and the wind

Table 2. Overview of the study area

Study area	Location	Type of coast	Date	Mean air temperature[1)]/°C	Mean wind speed[2)]/m·s^{-1}	Mean water depth[3)]/m
Bayuquan	eastern Liaodong Gulf	rocky coast	2016–10–29	8.12	1.10	4.50
Nanpaihe	western Bohai Gulf	silty coast	2016–12–09	5.78	3.08	3.50
Bayuquan	eastern Liaodong Gulf	rocky coast	2017–02–12	–0.80	2.86	4.00

Note: [1)2)3)] The data were obtained by *in situ* observations.

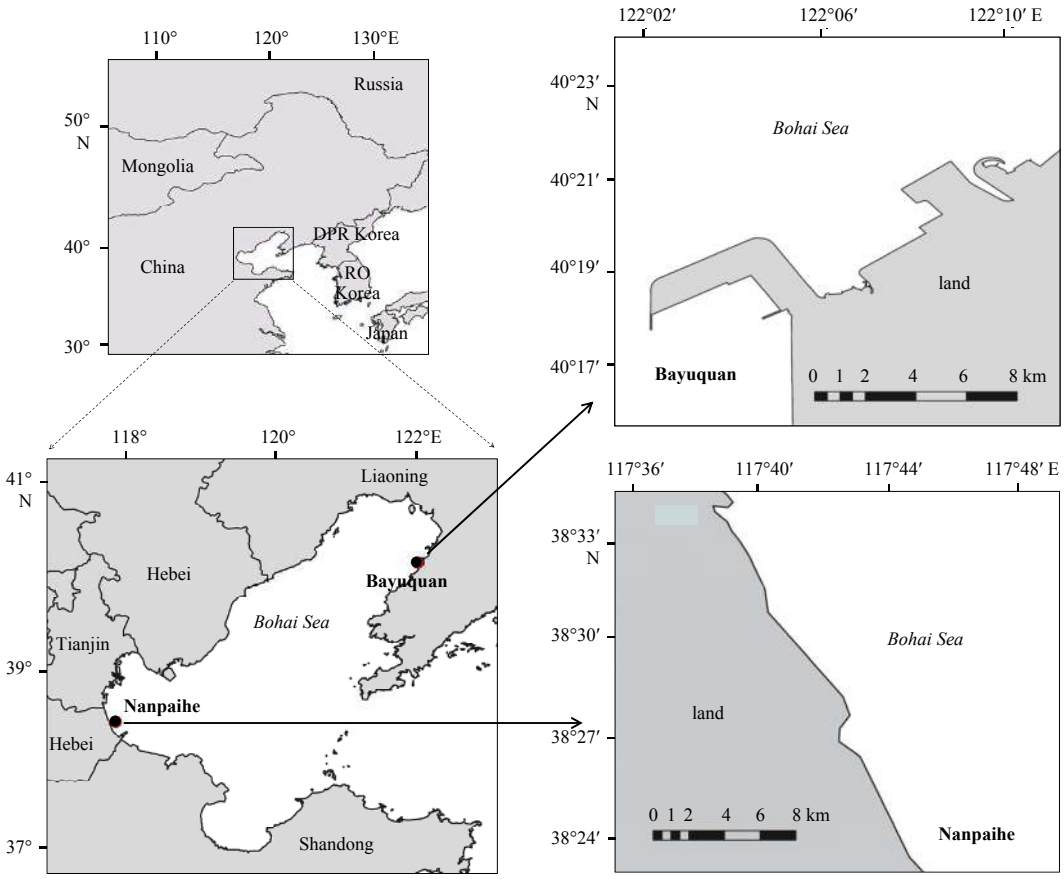

Fig. 3. Maps of the study area.

speed are shown in Fig. 5. The modelled ice velocity, the current velocity, and the wind speed are listed in Table 3. In Bayuquan, the trajectories of the modelled ices A and B were close and the average velocity of A was slightly larger than B. Both A and B mainly drifted towards the southeast, with some movements in the south and southwest. The average current velocity in Bayuquan was slightly smaller than the modelled ice velocity. The current moved mostly toward the east, sometimes toward the southeast and the southwest. The wind speed was extremely small with light air forced during the observation period; the west wind was predominant, followed by the southeast and east winds. In Nanpaihe, the trajectories of the modelled ices A, B, and C were also close and the average velocity of modelled ice followed the decreasing order of A greater than B greater than C. The main drift direction of these three modelled ices was northeast and the secondary direction was north. The average current velocity in Nanpaihe was slightly larger than the modelled ice velocity and the main current direction was northeast, sometimes northwest. A gentle breeze was responsible for a wind speed of (5.19±1.08) m/s; the southwest wind was prevailing, followed by the west wind.

The ice drift was consistent with the current velocity change, showing notable drift characteristics following the current flow (Fig. 5). The velocity of the modelled ices A and B gradually decreased with decreasing current velocity during the experimental time in 29 October 2016 (Fig. 5a). Figure 5b shows that the current direction reverses from 08:40 to 09:20 am on 8 December 2016; the direction of the modelled ice drift also changes. The current velocity gradually increased from 09:53 to 10:27 am and the ice drift velocity also increased. Thus the current in the Bohai Sea played an important role in the modelled ice drift.

Although the wind was mild during the observation period, the wind also played a certain role in the modelled ice drift. When the direction of the wind and modelled ice were the same, the modelled ice drift was accelerated, forced by the wind. When the current direction was in conversion after 15:33 on 29 October 2016 (Fig. 5a), the modelled ice velocity gradually increased under the action of the wind with the same direction in Bayuquan. When the wind direction was opposite to that of the modelled ice, however, the modelled ice velocity decelerated due to the wind. From 15:16 to 15:32 on 29 October 2016 (Fig. 5a), the ice drift velocity decreased and the direction then changed due to the increased opposite wind. The average velocity (15.8 cm/s) of the ocean currents from 11:03 to 11:07 on 12 February 2017 was

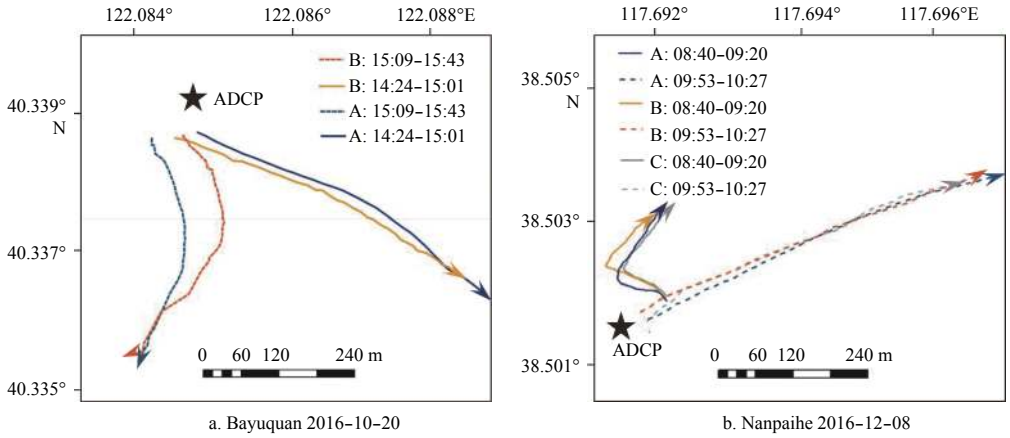

a. Bayuquan 2016–10–20 b. Nanpaihe 2016–12–08

Fig. 4. Trajectories of modelled ices in Bayuquan (a) and Nanpaihe (b) during the non-frozen period.

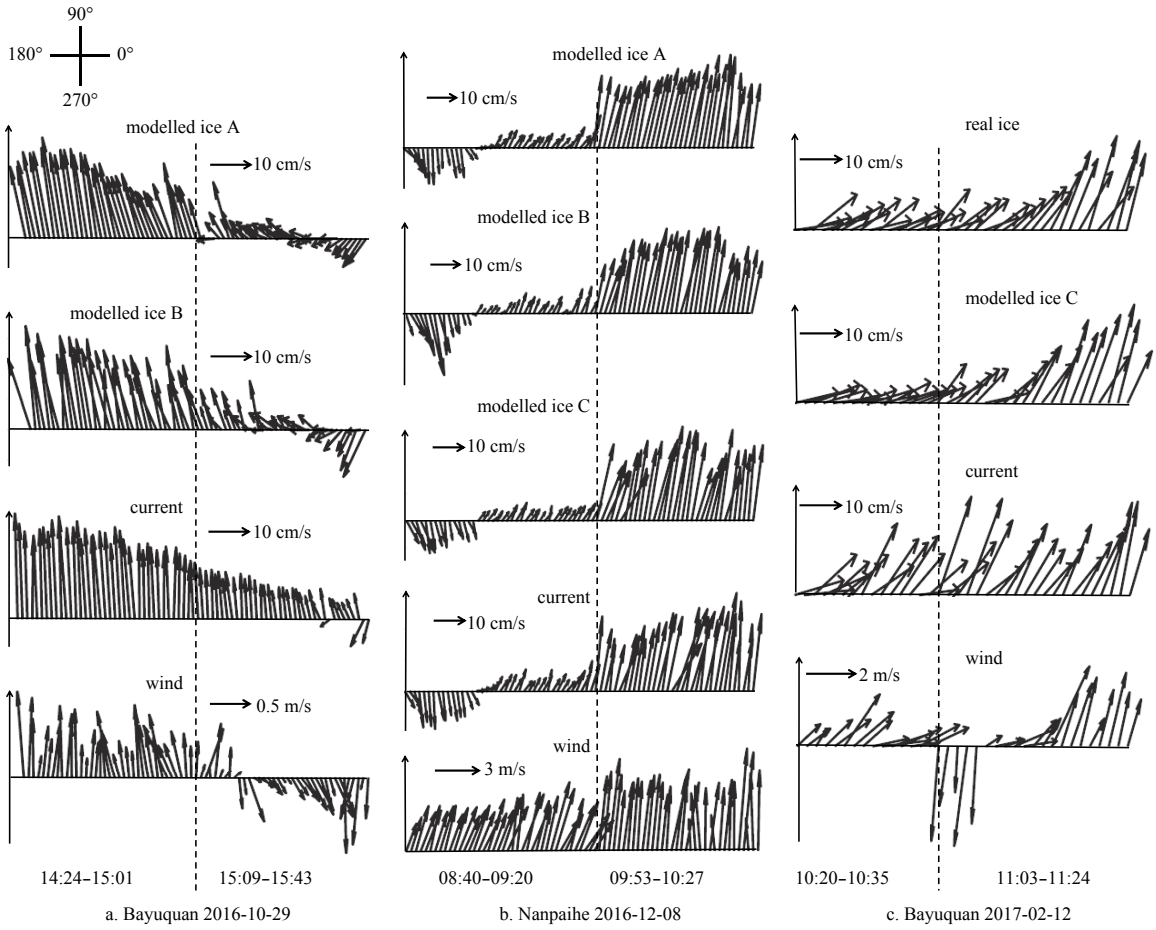

a. Bayuquan 2016-10-29 b. Nanpaihe 2016-12-08 c. Bayuquan 2017-02-12

Fig. 5. Vectors of the modelled ice velocity, current velocity, and wind speed in the Bohai Sea.

Table 3. Summary of the modelled ice velocity, current velocity, and wind speed

Location	Modelled ice	Sample number	Modelled ice velocity/cm·s^{-1}	Current velocity/cm·s^{-1}	Wind speed/cm·s^{-1}
Bayuquan	A	73	6.20–25.82(16.30±4.33)	6.17–25.23(14.34±6.07)	0.13–2.15(0.61±0.27)
Bayuquan	B	73	6.12–24.37(15.13±5.04)		
Nanpaihe	A	74	5.79–31.95(16.56±8.73)	7.03–38.20(17.35±9.19)	2.50–8.20(5.19±1.08)
Nanpaihe	B	74	3.43–31.23(15.52±9.02)		
Nanpaihe	C	74	4.86–29.76(14.90±8.22)		

larger than before (Fig. 5c); however, the modelled ice velocity decreased due to the wind with the opposite direction, which indicates that the wind with the opposite direction decelerates the ice drift velocity.

To sum up, the currents played a major role while the wind played a minor role in the free drift of isolated modelled ice in the Bohai Sea when the wind is mild. Previous studies have also reported that the wind plays a minor role in the free drift when it is mild. Zhang (1986) concludes that when the wind speed is larger than 10.8 m/s, the sea ice drift in the Bohai Sea is mostly controlled by the wind, and the sea ice drift direction is more closer to the wind direction with higher wind speed. When the wind speed is lower than 5.4 m/s, the ice velocity is generally close to the current speed. Wu et al. (2005) had also found that the currents play a controlling role in the free drift with mild wind forcing.

3.2 *Impact of current and wind on modelled ice drift*

To investigate the impact of the current and the wind on the modelled ice drift, a multiple linear regression was employed. A time-varying isolated modelled ice velocity is balanced with the current and wind and the relationship between the ice drift, the currents, and the wind (Lang et al., 2014; Li and Lu, 2006; Wu et al., 2005) can be described as follows:

$$\begin{bmatrix} I_1 \\ I_2 \\ \vdots \\ I_n \end{bmatrix} = \begin{bmatrix} C_1 & W_1 & 1 \\ C_2 & W_2 & 1 \\ \vdots & \vdots & \vdots \\ C_n & W_n & 1 \end{bmatrix} \begin{bmatrix} a \\ b \\ c \end{bmatrix}, \tag{1}$$

$$\begin{bmatrix} a \\ b \\ c \end{bmatrix} = \begin{bmatrix} C_1 & W_1 & 1 \\ C_2 & W_2 & 1 \\ \vdots & \vdots & \vdots \\ C_n & W_n & 1 \end{bmatrix}^{-1} \begin{bmatrix} I_1 \\ I_2 \\ \vdots \\ I_n \end{bmatrix}, \tag{2}$$

where I, C and W are the ice velocity, current velocity and wind speed, respectively, and these three parameters are all complex numbers; n is the number of the sea ice drift vectors in the formula; the weighted coefficients of the current and wind of the modelled ice drift are a and b, respectively; and c is a constant. The multiple regression parameters of the modelled ice drift in different zones in the Bohai Sea are listed in Table 4. The number of the sea ice drift vectors represents the number of the group of ice–current–wind vector data. Notably, two kinds of modelled ices (A and B) and three kinds of modelled ices (A, B and C) were used in the Bayuquan and Nanpaihe, respectively.

The multiple regression analysis provides the relationship among the ice velocity ($\vec{V}_{\rm i}$), current velocity ($\vec{V}_{\rm c}$), and wind speed ($\vec{V}_{\rm w}$) as follows:

$$\begin{aligned} \vec{V}_{\rm i,\,Ba} = {} & 0.856\ 0{\rm e}^{{\rm i}(-3.36)}\vec{V}_{\rm c} + \\ & 0.022\ 7{\rm e}^{{\rm i}(34.39)}\vec{V}_{\rm w} - 0.083\ 9{\rm e}^{{\rm i}(70.63)}, \end{aligned} \tag{3}$$

$$\begin{aligned} \vec{V}_{\rm i,\,Nan} = {} & 0.768\ 8{\rm e}^{{\rm i}(-6.79)}\vec{V}_{\rm c} + \\ & 0.009\ 2{\rm e}^{{\rm i}(82.49)}\vec{V}_{\rm w} + 0.034\ 0{\rm e}^{{\rm i}(-40.58)}. \end{aligned} \tag{4}$$

The correlation coefficients r^2 of the equations are 0.73 and 0.85, with a 0.01-significance level in Bayuquan and Nanpaihe, respectively. The equations of the multiple linear regression reflected the relationship among the ice drift velocity, the current velocity, and the wind speed well, indicating that the ice drift is significantly correlated with the current and the wind. The current coefficients were much larger than the wind, indicating that the influence of the ocean current on the ice drift is more significant than that of the wind. These results are in agreement with the result of previous studies (Lang et al., 2014; Li and Lu, 2006; Shi et al., 2016). In addition, the differences between the modelled ice drift and the current directions in Bayuquan and Nanpaihe were –3.36° and –6.79°, respectively, while that between the modelled ice drift and the wind directions were 34.39° and 82.49°.

To further explore the ice–current–wind relationship, the observed average current velocity and wind speed in Bayuquan on 29 October 2016 and Nanpaihe on 8 December 2016 were regarded as variables and substituted into the multiple regression equation. The calculated results are shown in Fig. 6. The ocean current plays a leading role in the ice drift when the wind is mild, no matter in Bayuquan or Nanpaihe. The calculated modelled ice velocity in Bayuquan was close to the observed velocity, with a magnitude error of 10.33% and direction error of 6.21°. The direction of the ice velocity in Bayuquan slightly shifted from the synthetic interval of the vector of the current and the wind with an acute angle (Fig. 6a). This suggests that the other factors, such as Coriolis force and pressure-gradient force has played a certain role in the free drift of isolated ice, especially in weak wind conditions, which is consistent with the findings of Fukamachi et al. (2011). The calculated modelled ice velocity in Nanpaihe was also close to the observed velocity, with a magnitude error of 12.05% and direction error of 4.78°. The direction of the ice velocity in Bayuquan was in the synthetic interval of the vector of the current and the wind (Fig. 6b). The contribution of other factors in Bayuquan is 0.083 9 in the multiple linear regression model, which is larger than that in Nanpaihe (Table 4). In addition to the difference of the Coriolis force and the pressure-gradient force, the different coefficients may be caused by the difference of the sample type and the number of the group of ice–current–wind vector data. Although there existed some differences, the ice velocity could still be estimated based on the current velocity and the wind speed when the *in situ* observed ice velocity was missing.

In addition, the effects of the current and the wind in this study were compared with previous studies, as listed in Table 5. The current coefficient of modelled ice in the Bohai Sea in this study is close to that of previous studies (0.640 0–1.320 0) in which data have been obtained by satellite or radar monitoring methods in different study areas, which indicates that the current plays a dominant role in the ice drift. The current coefficient, however, ranges widely due to the spatial difference of the current and the methods used to obtain the ice and current velocities. The ice velocity was calculated from remote sensing data in most studies (Lang et al., 2014; Li and Lu, 2006; Shi et al., 2016;

Table 4. Multiple regression parameters of the modelled ice drift in different zones

Location	n	Current coefficient	Wind coefficient	Constant	r^2	F	P	Standard residual
Bayuquan	146	$0.856\ 0{\rm e}^{{\rm i}(-3.36)}$	$0.022\ 7{\rm e}^{{\rm i}(34.39)}$	$-0.083\ 9{\rm e}^{{\rm i}(70.63)}$	0.73	194.52	<0.01	0.002 1
Nanpaihe	222	$0.768\ 8{\rm e}^{{\rm i}(-6.79)}$	$0.009\ 2{\rm e}^{{\rm i}(82.49)}$	$0.034\ 0{\rm e}^{{\rm i}(-40.58)}$	0.85	635.01	<0.01	0.002 4

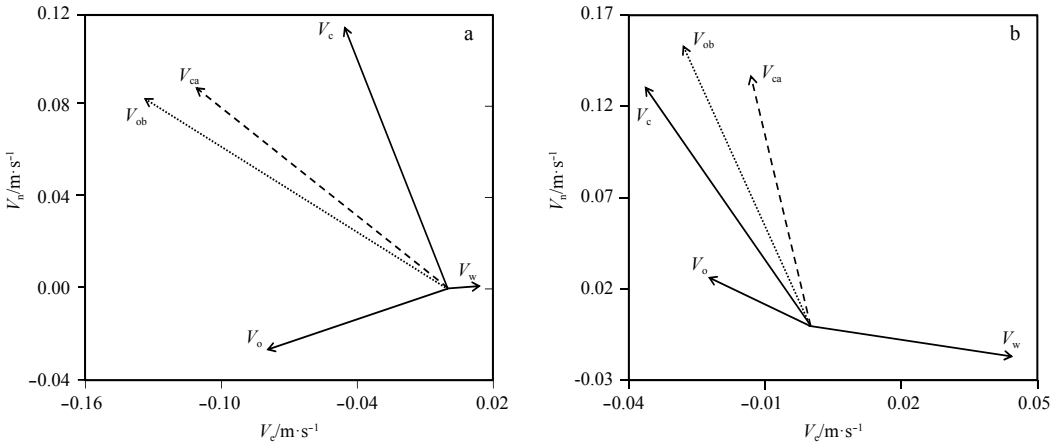

Fig. 6. Relationships among modelled ice, current and wind in Bayuquan (a) and Nanpaihe (b). V_{ca} is the calculated modelled ice drift velocity based on the multiple linear regression model; V_{ob} is the observed modelled ice drift velocity; V_c, V_w and V_o are the current velocity, the wind speed, and the velocity influenced by other factors, respectively; V_n is the north velocity, and V_e is the east velocity.

Table 5. Comparison of multiple regression parameters among different studies

Object	Location	Method (ice–current–wind)	Current coefficient	Wind coefficient	Reference
Modelled ice	Liaodong Gulf	*in situ–in situ–in situ*	0.856 0	0.025 7	this study
Modelled ice	Bohai Gulf	*in situ–in situ–in situ*	0.768 8	0.009 2	this study
Ice zone	Bohai Sea	satellite–model–model	1.320 0	0.022 0	Wu et al. (2005)
Ice zone	Bohai Sea	satellite–model–model	0.912 4	0.025 5	Lang et al. (2014)
Ice zone	Liaodong Gulf	laser rangefinder–*in situ–in situ*	0.780 0	0.040 0	Shi et al. (2016)
Iceberg	Labrador	ship radar–*in situ–in situ*	0.640 0	0.017 0	Smith (1993)
Iceberg	Antarctic Ocean	ship radar–*in situ–in situ*	0.813 8	0.017 4	Li and Lu (2006)

Smith, 1993; Wu et al., 2005). Some researchers retrieved the current velocity from ocean models (Lang et al., 2014; Wu et al., 2005). The above-mentioned non-contact measured data might have an effect on the difference of the current coefficient. The wind coefficient of modelled ice was close to or slightly smaller than that (0.013 0–0.040 0) of previous studies. The difference of the wind coefficient between this study and previous studies was also related to unmeasured data, which differed from the measured data such as reanalysis wind data (Lang et al., 2014; Wu et al., 2005). Accordingly, the *in situ* synchronous observations of ice–current–wind are important for the study of the ice drift characteristics, which can help to accurately determine the current and wind coefficients and provide key parameters for the numerical simulation of the ice drift (Fukamachi et al., 2011; Li et al., 2007).

3.3 *Comparison of drift of modelled ice with different density and thickness*

The drift characteristics of the modelled ice differ due to various densities and thicknesses, which can be seen in Table 3. The average ice velocity ((16.56±8.73) cm/s) of A with a smaller thickness was larger than that ((14.90±8.22) cm/s) of C when the densities of A and C were same. When the modelled ices B and C had the same thickness, the average ice velocity ((15.52±9.02) cm/s) of B was slightly larger than that ((14.90±8.22) cm/s) of C. Meanwhile, a smaller average ice velocity was found in heavier modelled ice. In addition, the differences of the drift of modelled ices with various densities and thicknesses were compared with the multiple regression model and the model parameters are listed in Table 6. The current and wind coefficients of modelled ice A (ρ=0.91 g/cm^3, h=4.0 cm) are greater than those of C (ρ=0.91 g/cm^3, h=7.0 cm), indicating that the modelled ice of the same density with smaller thickness is more sensitive to the current velocity and the wind speed changes. The current and wind coefficients of modelled ice B (ρ=0.81 g/cm^3, h=7.0 cm) are greater than those of C (ρ=0.91 g/cm^3, h=7.0 cm), indicating that the modelled ice of the same thickness with smaller density is more sensitive to the current velocity and the wind speed changes.

To further estimate the dependence on the ice density and thickness, we compared the above experiment results with the theoretical studies of Leppäranta (1998, 2005). For the case with the mild wind, we should retain the Coriolis and pressure gradient terms in the steady-state balance of forces for the sea ice drift (Fukamachi et al., 2011). Leppäranta (1998, 2005) derived a theoretical curve showing that the wind factor decreased as R, a measure of the importance of the Coriolis and pressure gradient terms, increased. Here R is equal to $(\rho_i h_i f)/(\rho_a C_a U_a)$, where ρ_i and ρ_a are the ice and air densities, h_i is ice thickness, f is the Coriolis

Table 6. Multiple regression parameters of ice drift among different types of modelled ice

Type	n	Current coefficient	Wind coefficient	Constant	r^2	F	P	Standard residual
A	147	$0.787\,3e^{i(-3.64)}$	$0.020\,2e^{i(45.40)}$	$-0.086\,9e^{i(80.93)}$	0.91	748.50	<0.01	0.002 0
B	147	$0.782\,5e^{i(-8.26)}$	$0.015\,5e^{i(55.49)}$	$0.064\,0e^{i(81.82)}$	0.86	446.90	<0.01	0.002 9
C	74	$0.714\,6e^{i(-5.15)}$	$0.007\,5e^{i(78.69)}$	$0.025\,2e^{i(-34.82)}$	0.84	190.06	<0.01	0.002 2

parameter, C_a is an air drag coefficient and U_a is the wind speed. In this study, R value of the modelled ice A was less than C because of the thickness difference ($h_A<h_C$, $\rho_A=\rho_C$), hence the wind factor of A was greater than C, therefore, the theoretical tendency of the wind factor was consistent with the experiment result. Comparably, R value of modelled ice B was less than C due to the density difference ($h_B=h_C$, $\rho_B<\rho_C$), hence the wind factor of B was greater than C, and the theoretical tendency of the wind factor was also agree with the experiment result.

3.4 *Comparison of drift between modelled ice and real ice*

The comparative free drift experiment between modelled ice and real sea ice was carried out in the frozen period of 2016/2017 in the Liaodong Gulf. Real sea ice (approximately 2 m×1 m×8 cm) was selected for the experiment (Fig. 1b), which was close to the modelled ice C. The density of the real ice was 0.86 g/cm^3. The trajectories of modelled ice and real ice were close (Fig. 7) and the average velocity ((15.11±2.07) cm/s) of the modelled ice was slightly smaller than that ((15.96±2.16) cm/s) of real ice. The drift difference between the modelled ice and real ice was relatively large from 11:03 to 11:24 (Fig. 7). During that period, the velocity (14.53 cm/s) of real ice was larger than that (13.77 cm/s) of modelled ice because of the decrease of real ice due to the melting process forced by the thermal factor. Both modelled and real ice drifted mainly towards the north, with some drifts toward the northeast. The average current velocity (14.54 cm/s) was slightly smaller than the modelled and real ice velocity; the current mostly moved toward the north, sometimes toward the northeast. The wind speed was small ((1.71±0.53) m/s), with light breezes forced during the experimental period; the south wind was predominant, followed by the east and east winds.

The ice–current–wind relationships of the modelled and real ice drifts were also established based on the multiple regression. The results are as follows:

$$\vec{V}_{\mathrm{mo,i}} = 0.807\,8e^{i(9.28)}\vec{V}_c + 0.010\,2e^{i(11.31)}\vec{V}_w + 0.022\,4e^{i(50.98)}, \quad (5)$$

$$\vec{V}_{\mathrm{re,i}} = 0.814\,2e^{i(10.22)}\vec{V}_c + 0.010\,2e^{i(7.33)}\vec{V}_w + 0.030\,0e^{i(55.73)}, \quad (6)$$

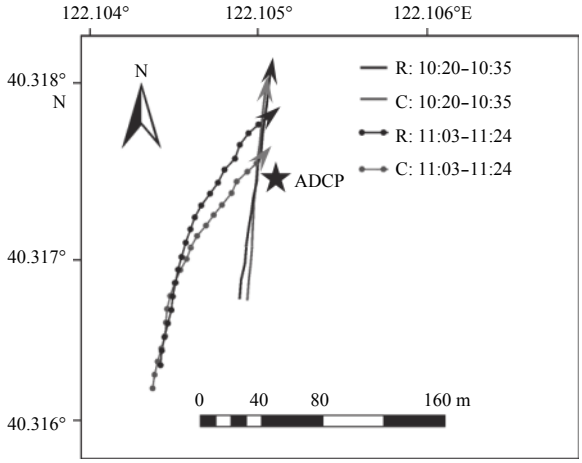

Fig. 7. Comparison of the trajectories of modelled ice C and real ice R.

where $\vec{V}_{\mathrm{mo,i}}$ and $\vec{V}_{\mathrm{re,i}}$ are the modelled ice and real ice drift velocities, respectively. The correlation coefficients r^2 of the equations for modelled and real ice were 0.73 and 0.76, respectively. The ice–current–wind relationship of the modelled ice was close to that of the real ice, with a 0.01 significance level, indicating that both real and modelled ice are significantly influenced by the current and the wind. The trajectories, the ice velocity, the current coefficient, the wind coefficient, and the constant of modelled ice were similar to those of the real sea ice; hence, the real ice could be substituted by modelled ice for *in situ* observations of the sea ice drift.

4 Conclusions

In this study, we used polypropylene material with a density similar to that of Bohai Sea ice as modelled ice and carried out a free drift experiment of modelled ice in the open sea in the Liaodong Gulf and the Bohai Gulf during the non-frozen period. We also conducted a comparative free drift experiment between the modelled and real sea ice in the Liaodong Gulf during the frozen period. The data of ice, current, and wind were obtained simultaneously during the non-frozen and frozen periods. The following conclusions were drawn.

(1) The simultaneous acquisition of the ice velocity, the current velocity, and the wind speed helps to understand the ice drift characteristics in the Bohai Sea. When the wind is mild in the Bohai Sea, the current plays a major role while the wind played a minor role in the free drift of isolated modelled ice.

(2) The modelled ice drift is significantly affected by the current and the wind based on the ice–current–wind relationship using the multiple linear regression. The magnitude error between the calculated and observed ice velocities is less than 12.05% and the velocity direction error is less than 6.21°. The ice velocity could be estimated using the observed current velocity and the wind speed when the observed ice velocity was hard to obtain.

(3) On the basis of the comparison of the difference of the drift of modelled ice with various densities and thicknesses, the same thickness with a smaller density is more sensitive to the current velocity and wind speed changes.

(4) The drift characteristics of modelled ice are similar to those of real sea ice, hence, the real ice can be substituted by modelled ice for *in situ* observations of the sea ice drift.

In this study, an *in situ* synchronous observation of ice–current–wind using modelled ice was developed and the modelled ice drift characteristics were investigated for a relatively short time. In the future, a longer experiment of the modelled ice drift will be conducted.

References

Bai Wei, Zhang Tong, McGovern D J. 2017. Response of small sea ice floes in regular waves: a comparison of numerical and experimental results. Ocean Engineering, 129: 495–506, doi: 10.1016/j.oceaneng.2016.10.045

Fukamachi Y, Ohshima K I, Mukai Y, et al. 2011. Sea-ice drift characteristics revealed by measurement of acoustic Doppler current profiler and ice-profiling sonar off Hokkaido in the Sea of Okhotsk. Annals of Glaciology, 52(57): 1–8, doi: 10.3189/172756411795931507

Gu Wei, Liu Chengyu, Yuan Shuai, et al. 2013. Spatial distribution characteristics of sea-ice-hazard risk in Bohai, China. Annals of Glaciology, 54(62): 73–79, doi: 10.3189/2013AoG62A303

Huang Guoxing, Law A W K. 2013. Wave-induced drift of large floating objects in regular waves. Journal of Waterway, Port, Coastal, and Ocean Engineering, 139(6): 535–542, doi: 10.1061/(ASCE)WW.1943-5460.0000207

Huang Guoxing, Law A W K, Huang Zhenhua. 2011. Wave-induced drift of small floating objects in regular waves. Ocean Engineering, 38(4): 712–718, doi: 10.1016/j.oceaneng.2010.12.015

Ji Shunying, Chen Xiaodong, Liu Yu, et al. 2013. Radar digital image technologies for the sea ice field observation based on an oil/gas platform and the measurement of the sea ice velocity. Haiyang Xuebao (in Chinese), 35(3): 119–127

King J C. 2003. Validation of ECMWF sea level pressure analyses over the Bellingshausen Sea, Antarctica. Weather and Forecasting, 18(3): 536–540, doi: 10.1175/1520-0434(2003)18<536:VOESLP>2.0.CO;2

Lang Wenhui, Wu Qing, Zhang Xi, et al. 2014. Sea ice drift tracking in the Bohai Sea using geostationary ocean color imagery. Journal of Applied Remote Sensing, 8(1): 083650, doi: 10.1117/1.JRS.8.083650

Leppäranta M. 1998. The Dynamics of Sea Ice. Helsinki: University of Helsinki Press

Leppäranta M. 2005. The Drift of Sea Ice. Berlin: Springer-Verlag

Li Zhijun, Lu Peng. 2006. Preliminary analysis of iceberg characteristics in the Antarctic Ocean. Journal of Dalian University of Technology (in Chinese), 46(3): 418–422

Li Zhijun, Zhang Zhanhai, Lu Peng, et al. 2007. Some parameters on arctic sea ice dynamics from the expedition in summer of 2003. Advances in Water Science (in Chinese), 18(2): 193–197

Lin Yebin, Xu Yingjun, Gu Wei, et al. 2010. Distribution of sea ice density and air porosity along the coast of the Bohai Sea. Resources Science (in Chinese), 32(3): 412–416

Liu Chengyu, Gu Wei, Chao Jinlong, et al. 2013. Spatio-temporal characteristics of the sea-ice volume of the Bohai Sea, China, in winter 2009/10. Annals of Glaciology, 54(62): 97–104, doi: 10.3189/2013AoG62A305

McGovern D J, Bai Wei. 2014. Experimental study on kinematics of sea ice floes in regular waves. Cold Regions Science and Technology, 103: 15–30, doi: 10.1016/j.coldregions.2014.03.004

Meylan M H, Yiew L J, Bennetts L G, et al. 2015. Surge motion of an ice floe in waves: comparison of a theoretical and an experimental model. Annals of Glaciology, 56(69): 155–159, doi: 10.3189/2015AoG69A646

Murray J, Guy G, Muggeridge D. 1983. Response of modelled ice masses to regular waves and regular wave groups. In: Proceedings of the International Conference on Oceans. San Fransisco: Institute of Electrical and Electronic Engineers, 1048–1052

Richter-Menge J A, Perovich D K, Elder B C, et al. 2006. Ice mass-balance buoys: a tool for measuring and attributing changes in the thickness of the arctic sea-ice cover. Annals of Glaciology, 44: 205–210, doi: 10.3189/172756406781811727

Robards M D, Silber G K, Adams J D, et al. 2016. Conservation science and policy applications of the marine vessel automatic identification system (AIS)—A review. Bulletin of Marine Science, 92(1): 75–103, doi: 10.5343/bms.2015.1034

Shi Wenqi, Yuan Shuai, Xu Ning, et al. 2016. Analysis of floe velocity characteristics in small-scaled zone in offshore waters in the eastern coast of Liaodong Bay. Cold Regions Science and Technology, 126: 82–89, doi: 10.1016/j.coldregions.2016.04.004

Simizu D, Ohshima K I, Ono J, et al. 2014. What drives the southward drift of sea ice in the Sea of Okhotsk?. Progress in Oceanography, 126: 33–43, doi: 10.1016/j.pocean.2014.05.013

Smith S D. 1993. Hindcasting iceberg drift using current profiles and winds. Cold Regions Science and Technology, 22(1): 33–45, doi: 10.1016/0165-232X(93)90044-9

Timmermans M L, Proshutinsky A, Krishfield R A, et al. 2011. Surface freshening in the Arctic Ocean's Eurasian Basin: an apparent consequence of recent change in the wind-driven circulation. Journal of Geophysical Research: Oceans, 116(C8): C00D03, doi: 10.1029/2011JC006975

Wake A, Poon Y K, Crissman R. 1987. Ice transport by wind, wave, and currents. Journal of Cold Regions Engineering, 1(2): 89–103, doi: 10.1061/(ASCE)0887-381X(1987)1:2(89)

Wu Longtao, Wu Huiding, Li Wanbiao, et al. 2005. Sea ice drifts in response to winds and tide in the Bohai Sea. Haiyang Xuebao (in Chinese), 27(5): 15–21

Yan Yu, Shao Dongdong, Gu Wei, et al. 2016. In-situ observation and three-dimensional numerical simulation of cooling water discharge from Bayuquan thermal power plant. Marine Environmental Science (in Chinese), 35(4): 571–579

Zhang Fangjian. 1986. Sea Ice in Our Country (in Chinese). Beijing: China Ocean Press